Structural Changes and Cation Site Ordering in Na and K Forms of Aluminogermanates with the Zeolite Gismondine Topology

Akhilesh Tripathi,*[,†] John B. Parise,[†,‡] Sun Jin Kim,[‡,⊥] Yongjae Lee,[‡] Geoffrey M. Johnson,[‡,||] and Young Sun Uh[⊥]

Department of Chemistry, State University of New York, Stony Brook, New York 11794-3400, Department of Geosciences, State University of New York, Stony Brook, New York 11794-2100, and Materials Chemistry Research Center, Korea Institute of Science and Technology, Cheongryang, Seoul 130-650, South Korea

Received June 6, 2000. Revised Manuscript Received September 29, 2000

Two new aluminogermanates, K−AlGe-GIS ($K_8Al_8Ge_8O_{32}\cdot 8H_2O$) and Na−AlGe-GIS ($Na_{24}Al_{24}Ge_{24}O_{96}\cdot 40H_2O$), with the zeolite gismondine (GIS) type framework topology have been synthesized hydrothermally and characterized using single-crystal X-ray diffraction. K−AlGe-GIS crystallizes in the monoclinic space group $I2/a$ with $a = 10.311(2)$ Å, $b = 9.749(1)$ Å, $c = 10.225(6)$ Å, $\beta = 90.000(2)°$, and $Z = 8$. Na−AlGe-GIS crystallizes in the monoclinic space group $C2/c$ with $a = 14.490(3)$ Å, $b = 9.940(2)$ Å, $c = 23.530(5)$ Å, $\beta = 105.90(3)°$, and $Z = 8$. Strict alternation of Ge and Al atoms over the framework sites lowers the symmetry of these aluminogermanates from their topological framework symmetry of $I4_1/amd$ to the real symmetry $I2/a$. Both structures consist of twisted double-crankshaft chains running along the *a* and *c* axes. In K−AlGe-GIS, potassium and water statistically occupy extraframework sites along the perpendicular eight-ring channels. In Na−AlGe-GIS, all three sodium sites are fully occupied and only three out of seven sites containing water are statistically occupied. A zigzag-ordered arrangement of Na sites in Na−AlGe-GIS results in unit cell symmetry hitherto unobserved for GIS. The synthesis of Na−AlGe-GIS requires the presence of organic bases, while K−AlGe-GIS can be synthesized from gels with or without organic bases. Time-resolved synchrotron X-ray powder diffraction patterns obtained as a function of temperature for Na−AlGe-GIS show a gradual disappearance of the *C*-centered cell between 150 and 180 °C with a simultaneous appearance of an *I*-centered monoclinic phase. Calculated powder diffraction patterns indicate that this phase change results from disordering of Na sites in the eight-ring channels. Results of a single-crystal diffraction study for a 50% Na-exchanged K−AlGe-GIS ($K_4Na_4Al_8Ge_8O_{32}\cdot 8H_2O$) shows that the space group $I2/a$ is retained with a 0.3% increase in the unit cell volume. Both the AlGe frameworks retain the GIS topology until ca. 750 °C after dehydration. The average Al−O−Ge (T−O−T) bond angle of 135.75° in K−AlGe-GIS and 135.29° in Na−AlGe-GIS is smaller than the average Al−O−Si bond angle of 145° in aluminosilicates.

Introduction

The substitution of Ge for Si in aluminosilicate materials can affect cation distribution. In the case of microporous materials this will influence the ion-exchange capacity, catalytic activity, and molecular-sieving properties.[1−4] Our initial results also demonstrate that such a substitution can produce mild as well as dramatic changes in cation distribution, thus influencing the overall structure. The distribution of extraframework cations is markedly different in low silica X (FAU) compared with the aluminogermanate analogue.[5a] Zeolite RHO provides a further case in point: AlSi−RHO possesses a Si/Al = 3, whereas in the aluminogermanate analogue, Ge/Al = 1.[5b,6] AlGe−RHO not only possesses an increased ion-exchange capacity

* To whom correspondence should be addressed. E-mail: atripath@ic.sunysb.edu.

† Department of Chemistry, State University of New York, Stony Brook.

‡ Department of Geosciences, State University of New York, Stony Brook.

§ Present address: Materials Chemistry Research Center, Korea Institute of Science and Technology, Cheongryang, Seoul 130-650, South Korea.

|| Present address: Department of Chemical Engineering, Worcester Polytechnic Institute, Worcester, MA 01609.

⊥ Korea Institute of Science and Technology.

(1) Helliwell, M.; Kaucic, V.; Cheetham, G. M. T.; Harding, M. M.; Kariuki, B. M.; Rizkallah, P. J. *Acta Crystallogr.* **1993**, *B49*, 413.

(2) Lerot, L.; Poncelet, G.; Fripiat, J. J. *J. Solid State Chem.* **1975**, *12*, 283.

(3) Breck, D. W. *Zeolite Molecular Sieves, Structure, Chemistry and Uses*; Wiley-Interscience: New York, 1974.

(4) Corma, A.; Martín-Aranda, R. M.; Sánchez, F. *J. Catal.* **1990**, *126*, 192.

(5) (a) Johnson, G. M.; Lee, Y.; Tripathi, A.; Parise, J. B. *Microporous Mesoporous Mater.* **1999**, *31*, 195. (b) Johnson, G. M.; Tripathi, A.; Parise, J. B. *Microporous Mesoporous Mater.* **1999**, *28* (1), 139. (c) Johnson, G. M.; Reisner, B. A.; Tripathi, A.; Corbin, D. R.; Toby, B. H.; Parise, J. B. *Chem. Mater.* **1999**, *11*, 2780. (d) Lee, Y.; Parise, J. B.; Tripathi, A.; Kim, S. J.; Vogt, T. *Microporous Mesoporous Mater.* **2000**, *39*, 445. (e) Tripathi, A.; Johnson, G. M.; Kim, S. J.; Parise, J. B. *J. Mater. Chem.* **2000**, *10*, 451. (f) Tripathi, A.; Kim, S. J.; Johnson, G. M.; Parise, J. B. *Microporous Mesoporous Mater.* **2000**, *34*, 273. (g) Johnson, G. M.; Tripathi, A.; Parise, J. B. *Chem. Mater.* **1999**, *11*, 10. (h) Tripathi, A.; Parise, J. B., unpublished work.

(6) Meier, W. M.; Olson, D. H.; Baerlocher, Ch. *Atlas of Zeolite Structure Types*, 4th ed.; Elsevier: London, 1996.

10.1021/cm000459s CCC: $19.00
Published on Web 11/18/2000

Table 1. Synthesis Conditions and Products

sample	gel composition[a]	product	form
A	$3.5K_2O:Al_2O_3:2GeO_2:85H_2O$	K−AlGe-GIS	crystalline powder
B	$3.5K_2O:Al_2O_3:3GeO_2:85H_2O$	K−AlGe-GIS	crystalline powder
C	$3.5K_2O:Al_2O_3:3GeO_2:85H_2O$	K−AlGe-GIS	crystalline powder
D	$5K_2O:Al_2O_3:4GeO_2:170H_2O$	K−AlGe-GIS	crystalline powder
E	$8K_2O:Al_2O_3:6GeO_2:170H_2O$	K−AlGe-GIS	twinned crystals
F	$20K_2O:Al_2O_3:15GeO_2:425H_2O$	K−AlGe-GIS	twinned crystals
G	$0.2LiO_2:5K_2O:Al_2O_3:4GeO_2:170H_2O$	K−AlGe-GIS	single crystals
H	$Na_2O:2K_2O:Al_2O_3:2GeO_2:85H_2O$	K−AlGe-GIS	crystalline powder
I	$Na_2O:K_2O:Al_2O_3:2GeO_2:85H_2O$	Na−AlGe-SOD + $KAlGeO_4$ + GIS	single crystals
J	$4R1:K_2O:Al_2O_3:5GeO_2:250H_2O$	K−AlGe-GIS	single crystals
K	$4R1:Na_2O:Al_2O_3:2GeO_2:200H_2O$	Na−AlGe-GIS + SOD[b]	single crystals
L	$2R1:Na_2O:Al_2O_3:2GeO_2:200H_2O$	Na−AlGe-GIS + SOD	single crystals
M	$R1:Na_2O:Al_2O_3:2GeO_2:200H_2O$	NAT[c]	single crystals
N	$4R1:Na_2O:Al_2O_3:5GeO_2:300H_2O$	NAT	single crystals
O	$4R1:Na_2O:Al_2O_3:2GeO_2:300H_2O$	no solids	
P	$6R2:Na_2O:Al_2O_3:2GeO_2:200H_2O$	NAT_{m1} + $Na−AlGe-GIS_{m2}$	crystalline powder
Q	$R3:Na_2O:Al_2O_3:2GeO_2:200H_2O$	NAT + Na−AlGe-GIS	crystalline powder
R	$3R3:Na_2O:Al_2O_3:2GeO_2:200H_2O$	Na−AlGe-GIS + NAT_{tr}	crystalline powder

[a] All gels except samples C and I were heated for 5 days at 110 °C. Sample C was heated for 2 days at 150 °C. Sample I was heated at 150 °C for 5 days. R1 = tetramethylammonium oxide [$(TMA)_2O$]. R2 = 1,4-diazabicyclo[2.2.2]octane (DABCO). R3 = tetraethylammonium oxide [$(TEA)_2O$]. [b,c] AlGe equivalents of zeolites with SOD and NAT topology. m1 = major product. m2 = minor product. tr = obtained in a trace amount only.

but it also shows appreciable distortion of the eight-membered rings, resulting in novel preferential cation siting for the lithium-exchanged derivative.[5c] Similarly, varying degrees of structural differences due to cation disposition have been observed in other aluminogermanates such as the ones with the zeolite CAN, NAT, ABW, JBW, MON, and ANA topology.[5d−h] Such a *topological dependence* illustrates the need to undertake a systematic investigation of aluminogermanates in order to incorporate a wide range of structure types.

The gismondine (GIS) topology is common to the minerals gismondine, garronite, gobbinsite, and amicite.[6] These and synthetic GIS typically possess variable Si/Al ratios. Further, several non-aluminosilicate variants are reported, including BeSi, MAPO, MAPSO, SAPO, ACP, GaSi, and with the usual variety of extraframework cations[5h,6] (Table I, given as Supporting Information; all of the tables and figures with Roman numerals have been deposited as Supporting Information). This accommodation of different compositions is ascribed to the high flexibility of the GIS topology.[7] Differentiation between the resultant wide range of symmetries, cation-ordering schemes, and sometimes subtle structural changes in these materials is difficult without high-quality diffraction data.[8]

We detailed the synthesis conditions for K−AlGe-GIS powder in a recent paper.[5g] The synthesis of single crystals of this material and Na−AlGe-GIS, together with the scattering contrast afforded by the combination of Ge and Al, prompted us for an unambiguous structure determination of these ordered variants of the GIS topology with Ge:Al = 1:1. The present work examines the structural changes, cation distribution, and ordering phenomena upon Ge substitution of Si in the GIS topology. Ion-exchange, in situ, and ex situ thermal studies are carried out to supplement this study.

Experimental Section

Synthesis. In a typical synthesis, single crystals of K−AlGe-GIS (sample G in Table 1) were obtained by dissolving a mixture of $LiOH·H_2O$ (0.043 g), KOH (1.60 g), and GeO_2 (1.04 g) in 7.05 g of deionized water. A total of 0.34 g of hydrated alumina ($Al_2O_3·2H_2O$; Catapal) was then added to this solution. After being stirred for 24 h at room temperature (RT), the resulting gel was allowed to crystallize at 110 °C for 5 days in a Teflon bottle. The solid products were filtered, washed with deionized water, and dried at RT. Translucent octahedral crystals were obtained. Although the general synthesis procedure for Na−AlGe-GIS is similar to that for K−AlGe-GIS, it can only be synthesized using a variety of organic amines (Table 1). Single crystals suitable for X-ray diffraction (sample J) were obtained by adding 25% (w/w) aqueous tetramethylammonium hydroxide (TMAOH; 7.29 g), NaOH (0.21 g), and GeO_2 (0.52 g) in 3.40 g of deionized water in a Teflon bottle. After complete dissolution, 0.34 g of hydrated alumina ($Al_2O_3·2H_2O$; Catapal) was added to this solution. The solution was stirred for 24 h at RT, and the resulting gel was allowed to crystallize at 100 °C for 5 days. The solid product was recovered by filtration, washed with deionized water, and dried at RT. Synthesis conditions for the preparation of K−AlGe-GIS and Na−AlGe-GIS are summarized in Table 1.

Characterization. The products obtained (Table 1) were characterized to establish phase identity and purity using a Scintag PAD-X automated X-ray powder diffractometer. Two types of crystals obtained in the case of Na−AlGe-GIS had zeolite GIS (octahedral) and SOD (cubic) type topology.[6] Wavelength-dispersive electron probe microanalysis (EPMA) was performed by a Cameca electron microprobe using an accelerating potential of 15 kV and a beam current of 10 nA. A 10 s counting time was employed to minimize the loss of Na.

Suitable single crystals were mounted on glass fibers, and data were collected on a Bruker Smart-CCD diffractometer equipped with a normal-focus X-ray tube (Mo Kα radiation, λ = 0.710 73 Å) operating at 50 kV and 30 mA. For each sample, a total of 1660 frames was

(7) Hansen, S.; Fälth, L.; Anderson, S. *J. Solid State Chem.* **1981**, *39*, 137.
(8) Hansen, S.; Håkansson, U.; Landa-Canovas, A. R.; Fälth, L. *Zeolites* **1993**, *13*, 276.

Table 2. X-ray Crystallographic Data Collection and Refinement Parameters for K−AlGe-GIS, Na−AlGe-GIS, and (K, Na)−AlGe-GIS[a]

name	K−AlGe-GIS	Na−AlGe-GIS	(K, Na)−AlGe-GIS
unit cell formula	$K_8Al_8Ge_8O_{32}\cdot 8H_2O$	$Na_{24}Al_{24}Ge_{24}O_{96}\cdot 40H_2O$	$K_4Na_4Al_8Ge_8O_{32}\cdot 8H_2O$
formula weight	1749.36	5197.92	1765.52
space group	*I*2/*a*	*C*2/*c*	*I*2/*a*
unit cell dimens (Å)	$a = 10.311(2)$, $b = 9.749(1)$, $c = 10.225(6)$, β (deg) = 90.000(2)	$a = 14.490(3)$, $b = 9.940(2)$, $c = 23.530(5)$, β (deg) = 105.90(3)	$a = 10.323(1)$, $b = 9.754(1)$, $c = 10.238(1)$, β (deg) = 90.01(2)
volume (Å^3)	1027.9(2)	3259(1)	1030.9(2)
no. of formula units per unit cell (Z)	8	8	8
calcd density (g cm^{-3})	2.826	2.613	2.714
absorption coefficient, μ (mm^{-1})	6.865	5.825	6.483
F(000)	832	2432	800
limiting indices	$-13 \le h \le 13$, $-12 \le k \le 12$, $-13 \le l \le 11$	$-18 \le h \le 18$, $-11 \le k \le 13$, $-30 \le l \le 30$	$-13 \le h \le 13$, $-12 \le k \le 12$, $-12 \le l \le 12$
crystal dimens (mm^3)	0.03 × 0.03 × 0.030	0.045 × 0.030 × 0.030	0.03 × 0.03 × 0.030
θ range (deg) and completeness to θ (%)	2.88−28.88, 94.5	1.80−28.03, 90.3	2.88−28.19, 90.7
reflcns collcd/unique/ $I > 2\sigma/R_{int}$	3654/1217/984/0.0504	9309/3579/1988/0.0633	3451/1159/966/0.0462
restraints/parameters	0/92	0/245	0/91
final R indices [$I > 2\sigma(I)$]	$R_1 = 0.0311$, w$R_2 = 0.0747$	$R_1 = 0.0465$, w$R_2 = 0.0822$	$R_1 = 0.0313$, w$R_2 = 0.0837$
final R indices (all data)	$R_1 = 0.0432$, w$R_2 = 0.0789$	$R_1 = 0.0990$, w$R_2 = 0.0929$	$R_1 = 0.0398$, w$R_2 = 0.0868$
goodness of fit on F^2 (GoF)	1.070	0.956	1.057
extinction coefficient	0.0005(4)	0.00013(3)	0.0000(5)
largest diff. peak and hole (e Å^{-3})	0.902 and −0.647	1.102 and −0.882	1.057 and −0.538

[a] $R_{int} = \sum(F_o^2 - F_o^2(\text{mean}))/\sum|F_o|^2$. $R_1 = \sum(||F_o| - |F_c||)/\sum|F_o|$. w$R_2 = \{\sum[w(F_o^2 - F_c^2)^2]/\sum[w(F_o^2)^2]\}^{0.5}$. $w = 1/[\sigma^2(F_o^2) + (0.0263P)^2 + 0.00P]$, where $P = (\text{Max}(F_o^2,0) + 2F_c^2)/3$. GoF $= [\sum w(F_o^2 - F_c^2)^2/\sum(n - p)]^{0.5}$.

collected at RT with a combination of ϕ and ω scans (width of ϕ and $\omega = 0.30°$ and exposure times of 60 s/frame for K−AlGe-GIS and 40 s/frame for Na−AlGe-GIS). Data were reduced using SAINT software,[9] and an empirical absorption correction was carried out using the program SADABS.[10] The structure was solved by direct methods followed by successive difference Fourier synthesis, with all calculations performed using SHELXTL.[11] Full-matrix least-squares refinements were against $|F^2|$. Anisotropic displacement factors were included for all of the atoms. No hydrogen atom positions were determined. Extraframework species were distinguished from each other based on their coordination environments and overall charge balances.

The systematic absences were consistent with either space groups *Ia* or *I*2/*a* for K−AlGe-GIS and either *Cc* or *C*2/*c* for Na−AlGe-GIS.[12] An inspection of the atomic coordinates obtained using the program PLATON[13,14] revealed that, after an origin shift in the acentric structure models was applied, pairs of atoms related by an inversion center can be found which fulfill the symmetry requirements of centric structure models within a maximal deviation of about five esd's for *I*2/*a* and four esd's for *C*2/*c*. Accordingly, the structures were refined in the centric space groups. Comparable residual factors were observed for both the acentric and the centric structure models (*Ia*, $R_1 = 0.0321$; *I*2/*a*, $R_1 = 0.0311$; *Cc*, $R_1 = 0.0463$; *C*2/*c*, $R_1 = 0.0465$).

In the case of K−AlGe-GIS, refinement of the individual site occupancies for the extraframework sites containing K1, K2, OW1, and OW2 resulted in occupancies of 42(2), 49.9(1), 70(4), and 57(3)%, respectively. In conjunction with an established empirical formula from EPMA and the derived separation distances of 0.758(8), 0.721(9), 2.22(1), and 2.15(2) Å between K1−OW1, K2−OW2, OW1A−OW1B, and OW2A−OW2B, respectively, these individual site occupancies were fixed to 50% in the final cycle of refinement. This resulted in a minor increase in R_1 from 3.0 to 3.1% (Table 2).

All Na sites are fully occupied in Na−AlGe-GIS. In an unconstrained refinement, two distinct site occupancies were observed for the water molecules; OW1, OW2, OW3, and OW4 sites were fully occupied, whereas OW5, OW6, and OW7 sites were partially occupied at 65.0(3), 44(5), and 55(2)% levels, respectively. Because of the close proximity of sites, OW5−OW6 [1.301(1) Å] and OW6−OW7 [0.845(2) Å], the site occupancies were fixed at the 50% level for the final refinement. In this case the value of R_1 increased from 4.63 to 4.65% (Table 2). Crystallographic results for K−AlGe-GIS and Na−AlGe-GIS are summarized in Table 2, while atomic coordinates, anisotropic displacement parameters, and selected bond distances and angles for K−AlGe-GIS and Na−AlGe-GIS are listed in Tables 3−6. A full list of the observed and calculated structure factors for K−AlGe-

(9) *SAINT: Program to integrate and Reduced Raw Crystallographic Area Detector Data*; Bruker AXS, Inc.: Madison, WI, 1996.
(10) Sheldrick, G. M. *SADABS, Siemens Area Detector Absorption Correction Program*; University of Göttingen: Göttingen, Germany, 1994.
(11) Sheldrick, G. M. *SHELXTL*; Bruker AXS Inc.: Madison, WI, 1997.
(12) Hahn, T., Ed. *International Tables for Crystallography A*, 3rd ed.; Kluwer Academic: Dordrecht, The Netherlands, 1992.
(13) Spek, A. L. *PLATON, A Multipurpose Crystallographic Tool*; Utrecht University: Utrecht, The Netherlands, 2000.
(14) Page, Y. L. *J. Appl. Crystallogr.* **1987**, *20*, 264; *J. Appl. Crystallogr.* **1988**, *21*, 983.

Table 3. Atomic Coordinates with Standard Uncertainties in Parentheses for K−AlGe-GIS

atom	site	p^a	x^b	y^b	z^b	$U_{11}{}^c$	$U_{22}{}^c$	$U_{33}{}^c$	$U_{23}{}^c$	$U_{13}{}^c$	$U_{12}{}^c$	$U_{eq}{}^d$
Ge1	8f	1.0	3745(1)	864(1)	3206(5)	10(1)	13(1)	9(1)	1(1)	1(1)	1(1)	11(1)
Al1	8f	1.0	745(1)	1603(1)	3750(1)	10(1)	12(1)	10(1)	2(1)	0(1)	−1(1)	11(1)
O1	8f	1.0	2068(1)	662(3)	3181(3)	9(2)	26(2)	34(2)	−2(1)	1(1)	4(1)	23(1)
O2	8f	1.0	4356(3)	−793(3)	3160(3)	13(2)	14(1)	28(2)	1(1)	−5(1)	5(1)	18(1)
O3	8f	1.0	4276(3)	1706(3)	1816(3)	30(2)	13(1)	11(2)	4(1)	6(1)	−2(1)	18(1)
O4	8f	1.0	4296(3)	1787(3)	4550(3)	32(2)	26(2)	8(2)	−4(1)	0(1)	−3(1)	22(1)
K1	8f	0.5	4087(4)	269(3)	−561(3)	70(2)	31(1)	24(1)	−4(1)	5(2)	−1(1)	42(1)
K2	8f	0.5	3054(3)	−2722(3)	1549(4)	32(2)	31(1)	98(3)	2(2)	−1(2)	−8(1)	54(1)
OW1	8f	0.5	3374(9)	131(12)	−441(12)	9(4)	87(8)	96(9)	−15(6)	1(5)	−7(5)	64(4)
OW2	8f	0.5	3093(17)	−2600(19)	855(9)	154(14)	168(14)	13(5)	16(7)	12(7)	67(10)	112(7)

[a] p = site occupancy. [b] Å × 10^4. [c] Anisotropic displacement factor given as Å^2 × 10^3 exp[$-2\pi^2\sum_j\sum_i h_1h_ja_ia_jU_{ij}$]. [d] Equivalent isotropic displacement parameters (Å^2 × 10^3) is defined as one-third of the trace of the orthogonalized U_{ij} tensor.

Table 4. Atomic Coordinates with Standard Uncertainties in Parentheses for Na−AlGe-GIS[a]

atom	site	p	x	y	z	U_{11}	U_{22}	U_{33}	U_{23}	U_{13}	U_{12}	U_{eq}
Ge1	8f	1.0	1362(1)	10934(1)	4760(1)	11(1)	11(1)	9(1)	0(1)	2(1)	−2(1)	11(1)
Ge2	8f	1.0	250(1)	6052(1)	3503(1)	11(1)	11(1)	10(1)	0(1)	4(1)	0(1)	11(1)
Ge3	8f	1.0	−1907(1)	9262(1)	3185(1)	11(1)	10(1)	10(1)	−1(1)	3(1)	1(1)	10(1)
Al1	8f	1.0	1512(2)	6568(2)	2604(1)	11(1)	9(1)	11(1)	2(1)	2(1)	2(1)	11(1)
Al2	8f	1.0	3249(2)	11346(2)	5906(1)	9(1)	11(1)	8(1)	0(1)	4(1)	0(1)	9(1)
Al3	8f	1.0	−134(2)	8697(2)	4253(1)	9(1)	11(1)	9(1)	0(1)	2(1)	0(1)	10(1)
O1	8f	1.0	1116(4)	6893(5)	3244(2)	17(3)	18(3)	11(3)	−4(2)	9(2)	−10(2)	14(1)
O2	8f	1.0	−2363	10749(4)	2817(2)	12(3)	13(2)	18(3)	0(2)	8(2)	1(2)	13(1)
O3	8f	1.0	−728(4)	5528(5)	2923(2)	13(3)	18(3)	7(3)	−1(2)	−3(2)	1(2)	14(1)
O4	8f	1.0	711(4)	4623(5)	3906(2)	14(3)	21(3)	16(3)	7(2)	2(2)	6(2)	17(1)
O5	8f	1.0	−1657(4)	8183(5)	2661(1)	17(3)	12(2)	18(3)	−6(2)	9(2)	1(2)	15(1)
O6	8f	1.0	−2710(4)	8482(5)	3518(2)	21(3)	19(3)	17(3)	2(2)	17(3)	−4(2)	17(2)
O7	8f	1.0	2519(4)	10769(5)	5231(2)	18(3)	21(3)	16(3)	−2(2)	1(2)	1(2)	19(1)
O8	8f	1.0	−865(4)	9771(5)	3719(2)	14(3)	14(3)	16(3)	−4(2)	−5(2)	−5(2)	17(1)
O9	8f	1.0	1057(4)	9343(5)	4429(2)	10(3)	13(2)	15(3)	−1(2)	3(2)	−3(2)	13(1)
O10	8f	1.0	1294(4)	12058(5)	4184(2)	15(3)	16(3)	11(3)	2(2)	6(2)	−1(2)	14(1)
O11	8f	1.0	−162(4)	7075(5)	3982(2)	21(3)	12(2)	14(3)	−5(2)	8(2)	−3(2)	15(1)
O12	8f	1.0	510(4)	11497(5)	5104(2)	15(3)	18(3)	11(3)	0(2)	6(2)	1(2)	15(1)
Na1	8f	1.0	−292(3)	13393(3)	4444(2)	25(2)	33(2)	38(2)	6(2)	11(2)	3(2)	32(1)
Na2	8f	1.0	2176(3)	8613(4)	3840(2)	34(2)	35(2)	33(2)	−4(2)	4(2)	7(2)	35(1)
Na3	8f	1.0	219(3)	11183(4)	3296(1)	34(2)	45(2)	21(2)	−8(2)	7(2)	−11(2)	34(1)
OW1	4e	0.5	0	9613(7)	2500	24(5)	17(4)	29(5)	0	13(4)	0	22(2)
OW2	8f	1.0	1922(4)	10593(6)	3278(2)	32(4)	38(3)	25(3)	−7(3)	16(3)	−5(3)	30(2)
OW3	8f	1.0	−1272(5)	13041(7)	3408(3)	56(6)	45(4)	60(5)	2(4)	−24(4)	−15(4)	62(2)
OW4	8f	1.0	−1158(6)	15314(7)	4541(4)	98(7)	43(4)	81(6)	26(4)	74(5)	35(4)	64(2)
OW5	8f	0.5	3281(8)	6994(10)	4397(5)	14(7)	10(5)	34(7)	5(5)	−1(6)	−1(5)	21(3)
OW6	8f	0.5	3162(12)	7771(19)	4787(9)	43(11)	95(14)	108(16)	50(13)	11(11)	32(11)	84(6)
OW7	8f	0.5	292(17)	12856(12)	2586(10)	120(30)	31(6)	21(13)	−2(7)	−22(11)	−11(9)	65(8)

[a] See footnotes in Table 3.

GIS and Na−AlGe-GIS can be obtained from the authors.

Thermogravimetric (TG) and differential thermal (DT) analyses were performed on the crystalline powder of both the AlGe samples using a SDT-2000/TA instrument between RT and 1000 °C under a flowing N_2 atm. A heating rate of 10 °C/min was used for all of the samples.

A powdered and single-crystal sample of K−AlGe-GIS was ion-exchanged with Na^+ using 0.5 M aqueous solutions of $NaNO_3$. In each case, 0.05 g of K−AlGe-GIS was contacted two times with 10 mL of an exchange solution and stirred for 20 h at RT. Atomic percentages obtained from EPMA indicated an exchange of ca. 45% K^+ by Na^+. A complete exchange by Na^+ ions was achieved by a 96 h treatment in a 0.5 M $NaNO_3$ solution at RT. However, agglomeration and high mosaicity rendered these materials unsuitable for single-crystal study. For the 45% ion-exchanged sample, partially occupied extraframework sites were also observed for Na and K in an unconstrained refinement. Based upon EPMA and the interatomic distance arguments similar to those described for K−AlGe-GIS above, the site occupancies of all of the extraframework species were

Table 5. Selected Interatomic Distances (Å) and Angles (deg) with Standard Uncertainties in Parentheses for K−AlGe-GIS

Ge1−O1	1.730(3)	Al1−O1	1.743(3)
Ge1−O2	1.735(3)	Al1−O2	1.743(3)
Ge1−O3	1.738(3)	Al1−O3	1.747(3)
Ge1−O4	1.740(3)	Al1−O4	1.749(3)
⟨Ge1−O⟩	1.735	⟨Al1−O⟩	1.745
O2−Ge1−O1	104.7(1)	O1−Al1−O2	106.8(2)
O2−Ge1−O4	112.6(1)	O1−Al1−O3	113.3(2)
O3−Ge1−O1	110.8(2)	O1−Al1−O4	113.8(2)
O3−Ge1−O2	107.7(1)	O2−Al1−O3	107.6(2)
O3−Ge1−O4	107.5(1)	O2−Al1−O4	111.7(2)
O4−Ge1−O1	113.2(1)	O3−Al1−O4	103.4(1)
⟨O−Ge1−O⟩	109.42	⟨O−Al1−O⟩	109.43
Ge1−O1−Al2	135.5(2)	Ge1−O3−Al2	135.6(2)
Ge1−O2−Al2	135.3(2)	Ge1−O4−Al2	136.5(2)
K1−O1	2.957(5)	K2−O3	3.269(5)
K1−O2	3.147(4)	K2−O4	2.993(5)
K1−O3A	2.812(4)	K2−OW1	3.34(1)
K1−O3B	2.864(4)	K2−OW2A	2.92(1)
K1−O4	2.880(4)	K2−OW2B	2.73(1)
K1−OW1A	2.74(1)		
K1−OW1B	2.83(1)		
K1−OW2	3.31(2)		

Table 6. Selected Interatomic Distances (Å) and Angles (deg) for Na−AlGe-GIS with Standard Uncertainties in Parentheses

Ge1−O7	1.745(5)	Ge3−O2	1.749(5)	Al2−O4	1.741(5)
Ge1−O9	1.763(5)	Ge3−O5	1.746(5)	Al2−O6	1.747(5)
Ge1−O10	1.738(5)	Ge3−O6	1.752(5)	Al2−O7	1.747(5)
Ge1−O12	1.745(5)	Ge3−O8	1.753(5)	Al2−O10	1.754(5)
⟨Ge1−O⟩	1.747	⟨Ge3−O⟩	1.750	⟨Al2−O⟩	1.747
Ge2−O1	1.750(5)	Al1−O1	1.783(5)	Al3−O8	1.764(5)
Ge2−O3	1.757(5)	Al1−O2	1.766(5)	Al3−O9	1.781(5)
Ge2−O4	1.737(5)	Al1−O3	1.768(5)	Al3−O11	1.746(5)
Ge2−O11	1.730(5)	Al1−O5	1.756(5)	Al3−O12	1.752(5)
⟨Ge2−O⟩	1.743	⟨Al1−O⟩	1.768	⟨Al3−O⟩	1.760
O10−Gel−O12	105.0(2)	O5−Ge3−O2	107.0(2)	O4−Al2−O7	108.5(3)
O10−Gel−O7	113.2(2)	O5−Ge(3)−O6	109.6(2)	O4−Al2−O6	113.4(3)
O12−Gel−O7	114.4(2)	O2−Ge(3)−O6	112.8(2)	O7−Al2−O6	116.7(3)
O10−Gel−O9	106.2(2)	O5−Ge(3)−O8	112.3(3)	O4−Al2−O10	101.6(3)
O12−Gel−O9	111.6(2)	O2−Ge3−O8	104.2(2)	O7−Al2−O10	110.0(3)
O7−Gel−O9	106.1(2)	O6−Ge3−O8	110.7(3)	O6−Al2−O10	105.6(3)
⟨O−Ge1−O⟩	109.41	⟨O−Ge3−O⟩	109.43	⟨O−Al2−O⟩	109.3
O11−Ge2−O4	105.5(2)	O5−Al1−O2	109.3(3)	O11−Al3−O(12)	103.4(3)
O11−Ge2−O1	111.0(2)	O5−Al1−O3	113.7(3)	O11−Al3−O8	110.9(3)
O4−Ge2−O1	112.1(2)	O2−Al1−O3	107.2(3)	O12−Al3−O8	114.4(3)
O11−Ge2−O3	109.2(2)	O5−Al1−O1	103.4(3)	O11−Al3−O9	110.2(3)
O4−Ge2−O3	106.8(2)	O2−Al1−O1	109.3(3)	O12−Al3−O9	110.4(3)
O1−Ge2−O3	112.0(2)	O3−Al1−O1	113.9(3)	O8−Al3−O9	107.5(3)
⟨O−Ge2−O⟩	109.43	⟨O−Al1−O⟩	109.46	⟨O−Al3−O⟩	109.46
Ge2−O1−Al1	129.4(3)	Ge2−O4−Al2	140.2(3)	Ge1−O7−Al2	141.6(3)
Ge3−O2−Al1	136.4(3)	Ge3−O5−Al1	151.8(3)	Ge3−O8−Al3	124.5(3)
Ge2−O3−Al1	126.8(3)	Ge3−O6−Al2	142.7(3)	Ge1−O9−Al3	122.4(3)
				Ge1−O10−Al2	137.1(3)
Na1−O4	2.493(6)	Na1−OW6	2.65(2)	Na3−O8	2.507(6)
Na1−O10	2.860(6)	Na2−O1	2.463(6)	Na3−O10	2.401(6)
Na1−O12	2.515(6)	Na2−O9	2.513(6)	Na3−OW1	2.391(6)
Na1−OW3	2.486(8)	Na2−OW2	2.342(7)	Na3−OW2	2.548(7)
Na1−OW4A	2.330(7)	Na2−OW3	2.76(1)	Na3−OW3	2.908(9)
Na1−OW4B	3.00(1)	Na2−OW5	2.39(1)	Na3−OW7A	2.38(2)
Na1−OW5	2.47(1)	Na2−OW6	2.44(2)	Na3−OW7B	2.60(2)

fixed to 50%. This resulted in a composition $Na_4K_4Ge_8Al_8O_{32}\cdot 8H_2O$ for (K, Na)−AlGe-GIS. Atomic coordinates and anisotropic displacement parameters are given in Table II as Supporting Information. A full list of bond lengths, bond angles, and the observed and calculated structure factors for (K, Na)−AlGe-GIS can be obtained from the authors.

To investigate the structural changes as a function of heating, high-temperature investigations were carried out using an imaging plate detector (Mar345, 2300 × 2300 pixels) and an in situ dehydration cell[15] at the X7B beamline of the National Synchrotron Light Source (NSLS). This allows the collection of time-resolved X-ray powder diffraction data and provides a real-time view of any transitions occurring as the sample is heated. A powdered sample (∼0.003 g) was loaded into a 0.7 mm quartz capillary, connected to a vacuum (<10 mTorr), and heated at a rate of 10 °C /min to 500 °C. The imaging plate was exposed for 120 s for each frame, and a readout time of ∼100 s was used for scanning and storing. The wavelength (λ = 0.9390 Å), sample-to-detector distance, zero point, and imaging plate (IP) tilt were determined using a LaB6 standard material prior to the experiment.[16] The temperature was calibrated using the known thermal expansion of an Ag standard. Data were integrated using FIT2D.[17,18]

(15) Norby, P. *Mater. Sci. Forum* **1996**, *147*, 228.
(16) Norby, P. *J. Appl. Crystallogr.* **1997**, *30*, 21.
(17) Hammersley, A. P. *FIT2D: V9.129 Reference Manual V3.1*; ESRF Internal Report ESRF98HA01T; ESRF: Grenoble, France, 1998.
(18) Hammersley, A. P. *J. Appl. Crystallogr.*, in press.

Results and Discussion

Structural Description and Comparison. The GIS topology, common to both of the AlGe frameworks, consists of two double-crankshaft chains of alternating GeO_4^{4-} and AlO_4^{5-} tetrahedra (T atoms), connected at right angles to each other to form a three-dimensional (3D) framework.[6,19] Its pores are interconnected through a 3D channel system with eight-ring openings along *a* and *c* axes. As a consequence of this arrangement of T atoms a gismondine-like cage is formed by four eight-membered and six four-membered rings.[6]

The average Ge−O and Al−O distances in K−AlGe-GIS are 1.735 and 1.745 Å, respectively, whereas for Na−AlGe-GIS, they are 1.747 and 1.758 Å, respectively. These distances compare well with the value 1.74 Å expected for Ge−O and Al−O bonds.[20] The ionic radii (*r*) of Al^{3+} and Ge^{4+} in tetrahedral coordination are the same (0.39 Å); hence, the Al/Ge ratio has no influence on the average T−O bond distance. As expected, an expansion of the unit cell is observed upon introduction of the larger germanium for silicon (Δr = 0.13 Å); the unit cell volume of K−AlGe-GIS is 5% larger than that of K−AlSi-GIS.[19] This expansion is moderated by a *reduction* in the Al−O−Ge framework bond angle. The decreasing values of average T−O−T angles for Na−AlSi-GIS,[19] K−AlSi-GIS,[19] K−AlGe-GIS, and Na−AlGe-GIS are 145°, 139°, 135.7°, and 135.2°, respectively. Thus, a greater degree of relative cell contraction is produced for AlGe materials compared with GaSi and

(19) Bauer, T.; Baur, W. H. *Eur. J. Mineral.* **1998**, *10*, 133.
(20) Shannon, R. D. *Acta Crystallogr.* **1976**, *A32*, 751.

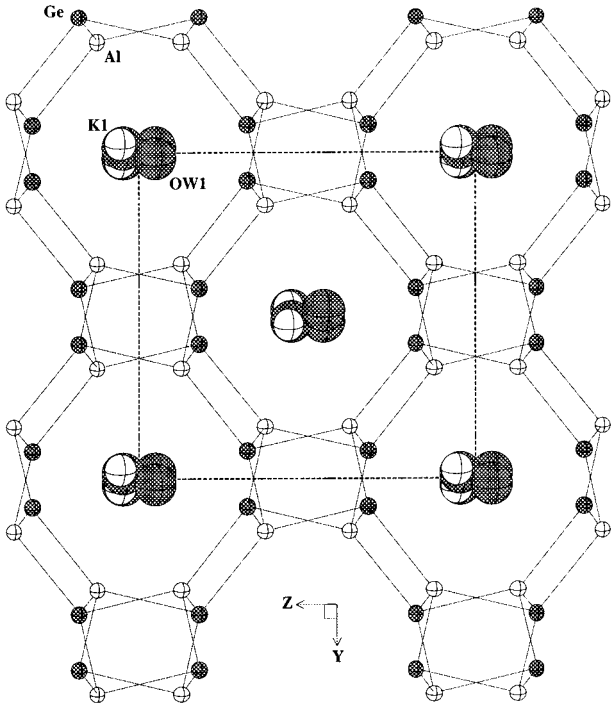

Figure 1. Projection along [100] for K−AlGe-GIS. Small empty spheres represent K ions, and dark spheres represent water molecules.

AlSi frameworks, an observation that is consistent with the isomorphous framework substitution of Ge in other topologies such as ABW, RHO, SOD, FAU, and NAT.[5a−h] The tetrahedra in both of the AlGe frameworks are regular, with deviation (standard deviations are computed using $s = 1/(N - 1)[\sum_{i=1}^{n}(\langle X\rangle_{\text{ideal}} - \langle X\rangle_i)^2]^{1/2}$) from the ideal tetrahedral angle (109.47°) for the Ge1 and Al1 tetrahedra being 3.30° and 4.15° in K−AlGe-GIS and 4.12°, 2.77°, 3.3° and 3.98°, 5.39°, 3.7° for Ge1, Ge2, Ge3 and Al1, Al2 and Al3 tetrahedra, respectively, in Na−AlGe-GIS.

The extraframework cations reside in the perpendicular eight-ring channels, and it is the ordering and dissimilarity in their distribution which results in the difference in symmetry of the two structures. In the case of K−AlGe-GIS, the disordered water molecules, occupying sites OW1 and OW2, as well as potassium at the sites K1 and K2 are statistically occupied. The sites K1 and OW1 are located close to the center of the eight-ring channels parallel to [100], whereas the sites K2 and OW2 are close to the center of the eight-ring channels parallel to [001] (Figures 1 and I given as Supporting Information). The sites K1 and K2 are coordinated to three half-occupied H_2O sites and five framework oxygen sites with interatomic distances in the range of 2.74(1)−3.31(1) and 2.73(1)−3.34(1) Å, respectively (Figure IIa,b given as Supporting Information). It is difficult to ascribe an exact coordination sphere for the K cations because of the disorder in the K and H_2O sites. The interatomic distances, ranging from 3.156 to 5.166 Å between the half-occupied H_2O sites, suggest a coordination sphere of 8 for both of the K cations. The sites OW1 and OW2 are coordinated to three K sites with interatomic distances in the range of 2.731(5)−3.404(6) and 2.743(6)−3.327(8) Å, respectively (Table 5). Unlike K−AlGe-GIS, the extraframework sites in Na−AlGe-GIS are ordered along the eight-ring channels. As shown in Figure 2a, the sites with Na cations arrange in a 3:1 zigzag, with Na1, Na2, and Na3 forming a row. In this arrangement the site with Na3 resides between the corners of the two four-membered rings of the parallel crankshaft chains. Another Na3 site is located diagonally opposite to this and forms the displaced parallel row with the other two Na sites, Na2 and Na1. On the other hand, both of the disordered Na sites in Na−AlSi-GIS[19] or in $Na_8Al_8Si_8O_{32}\cdot 15.2H_2O$ (LS−NaP)[21] when viewed along [010], can be described as forming a 1:1 zigzag arrangement (Figure 2b). This unique ordered arrangement of Na sites gives rise to a larger unit cell. The unit cell relations for K−AlSi-GIS,[19] Na−AlSi-GIS,[19] K−AlGe-GIS, and LS−NaP [the unit cell of (LS−NaP)[21] reported in the standard *C*-centered cell is related to the common *I*-centered cell with the space group *I*2/*a* (e.g., K−AlGe-GIS) by the relations $a' \cong \sqrt{2}a$, $b' \cong b$, and $c' \cong c$, where a' and a are the unit cell dimensions of LS−NAP and K−AlGe-GIS, respectively; a nonstandard setting (*I*2/*a*) is chosen for consistency with the previously reported GIS structures in the literature; this gives the view of the perpendicular eight-ring channels along the *a* and *c* axes] are shown in Figure 3. The minor increases in the cell dimensions of the AlGe-GIS materials result from the isomorphous substitution of Si by the larger Ge.

The two perpendicular eight-ring channels in Na−AlGe-GIS cannot be viewed along [001] and [100] when the monoclinic *C*-centered cell is converted to the *I*-centered cell (with the *b* axis being unique) using the transformation matrix (0, 0, −1; 0, 1, 0; 1, 0, −1) because the monoclinic angle β equals 144.53°.[13] The *I*-centered GIS topologies in the literature have $\beta \cong 90°$ (Table I). Accordingly, for an analogy with other GIS topologies, the two eight-ring channels in the original *C*2/*c* setting were viewed along [$\bar{1}$01] and [201] (Figures 4 and III given as Supporting Information). The three Na sites are close to the walls of the eight-ring channels. Sites Na1 and Na3 are coordinated to three framework oxygen sites, three fully occupied H_2O sites, and two half-occupied water sites with interatomic distances in the range of 2.330(7)−3.00(1) and 2.38(2)−2.908(9), respectively (Table 6). The interatomic distances between the statistically occupied H_2O sites are in the range of 2.330(7)−3.00(1) Å (Figure IV4a,c given as Supporting Information). The Na2 site is coordinated to two framework oxygen sites, three fully occupied sites, and two half-occupied H_2O sites with interatomic distances in the range of 2.342(7)−2.76(1) Å (Table 6 and Figure IVb given as Supporting Information). The sites OW1, OW2, and OW4 are close to the center of the eight-ring channels along [201], while the sites OW3, OW5, OW6, and OW7 are close to the center of the eight-ring channels along [$\bar{1}$01]. As explained in the structure refinement section, all of the half-occupied H_2O sites are disordered with unacceptable interatomic distances between the O atoms of the water molecule. Accordingly, all of the H_2O sites cannot be simultaneously coordinated to the Na sites. As a result, a coordination sphere of 7, 6, and 7 can be assigned to the sites containing Na1, Na2, and Na3, respectively (Figure IVa−c given as Supporting Information).

(21) Albert, B. R.; Cheetham, A. K.; Stuart, J. A.; Adams, C. J. *Microporous Mesoporous Mater.* **1998**, *21*, 133.

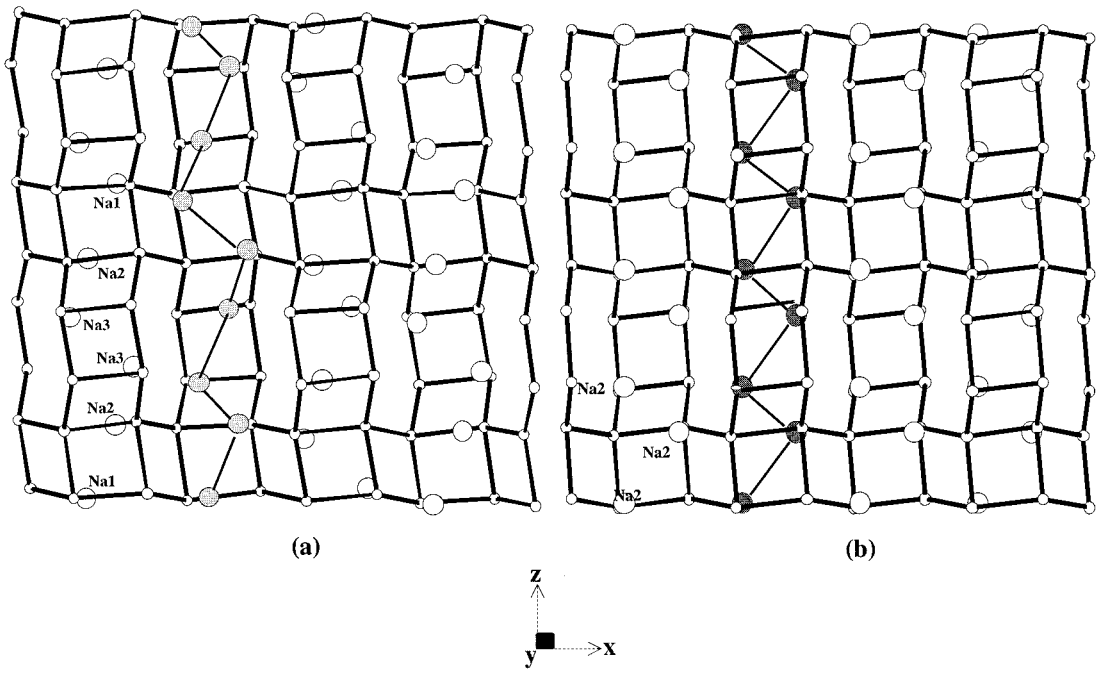

Figure 2. Projection along [010] of the structures of **(**a**)** Na−AlGe-GIS and **(**b**)** Na−AlSi-GIS.[19] The 3:1 and 1:1 zigzag arrangements of the sodium in Na−AlGe-GIS and Na−AlSi-GIS, respectively, have been highlighted. In the case of Na−AlSi-GIS only Na2 cations are shown because Na1 and Na2 are disordered in the eight-ring channel sites. Na1 resides near the center of the other two corners of the crankshaft chain in a fashion similar to that shown for Na2 in this projection. The water molecules are not shown for clarity.

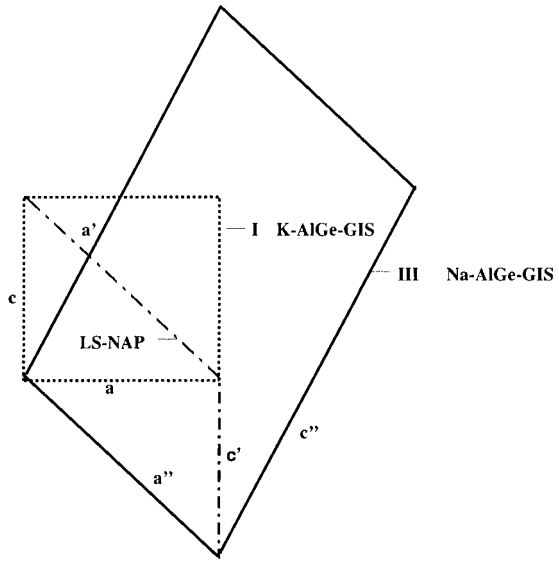

Figure 3. Relationships between the unit cells of K−AlGe-GIS (I), LS−NaP[21] (II), and Na−AlGe-GIS (III). The unit cells of I and II are different settings of the same monoclinic symmetry. The unit cell volume of III is 3 times that of I with the relationships $a'' \cong \sqrt{2}a$, $b'' \cong b$, and $c'' \cong \sqrt{5}c$.

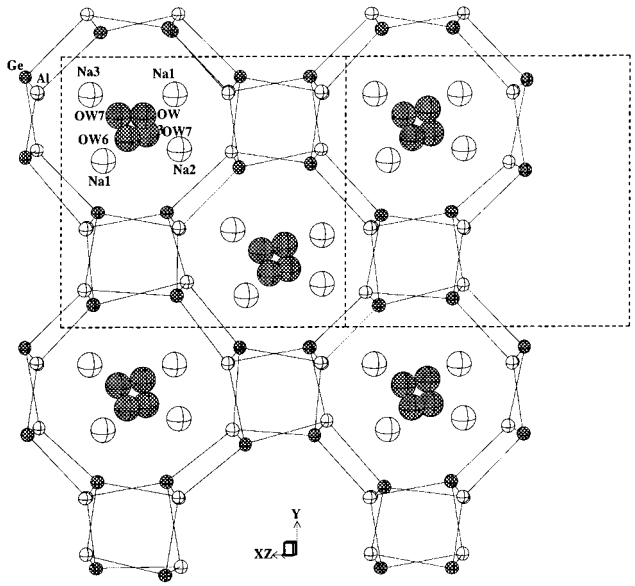

Figure 4. Projection along [$\bar{1}$01] of Na−AlGe-GIS. Empty spheres represent Na ions, and dark spheres represent water molecules.

We believe that the ordered arrangement of the sodium sites in Na−AlGe-GIS is due to the coordination sphere requirements arising from the twisting of the perpendicular crankshaft chains. A measure of this twisting is the distortion of the framework of GIS topology. The ratio of the longest (L) to the shortest diagonals (S) of an eight ring defines the ellipticity with values of L/S ratios of close to 1 for circular eight rings[22] (Figure V given as Supporting Information). The eight rings in both of the AlGe frameworks were found to be elliptically distorted with L/S = 1.81 for K−AlGe-GIS and 1.49 for Na−AlGe-GIS compared with L/S = 1.68 for K−AlSi-GIS and 1.41 for Na−AlSi-GIS.[19] This twisting creates suitable pockets that suits the coordination number and allows bonding of Na atoms with the oxygen atoms of the framework along the walls of the eight-ring channel system in an ordered fashion as against relatively less buckled channels in Na−AlSi-GIS (Figure 5). An attempt to put the Na cations at sites similar to those in Na−AlSi-GIS, which has relatively less buckled channels, resulted in unacceptable inter-

(22) Vezzalini, G.; Alberti, A.; Sani, A.; Triscari, M. *Microporous Mesoporous Mater.* **1999**, *31*, 253.

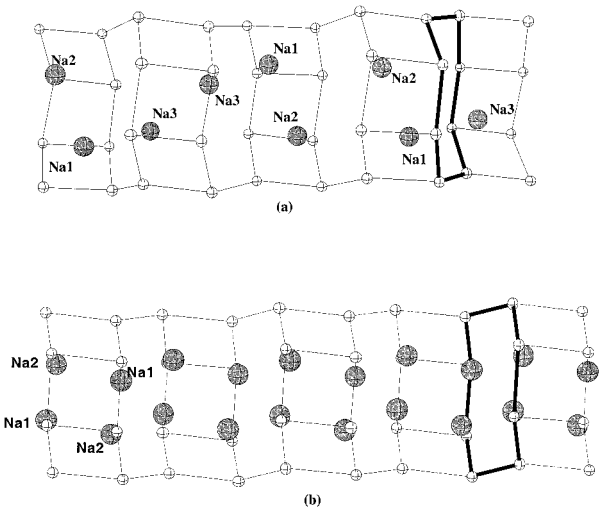

Figure 5. Nodal representation of the crankshaft chains in (a) Na−AlGe-GIS and in (b) Na−AlSi-GIS[19] viewed approximately parallel to [010]. Large dark spheres represent Na, while small empty spheres represent the framework Ge/Si/Al atoms. The highlighted portion shows more buckled chains in Na−AlGe-GIS compared to Na−AlSi-GIS. Water molecules are omitted for clarity.

atomic distances among the Na cations. In the case of K−AlGe-GIS, the larger K sites are close to the *center* of eight-ring channels, which suits their coordination requirements. An ordered arrangement of K is ruled out at these sites because this would result in unacceptable bond distances among the K sites despite highly buckled crankshaft chains in K−AlGe-GIS.

For gels with composition $K_2O/GeO_2 > 1$, a highly crystalline powdered form of K−AlGe-GIS is obtained for a large range of GeO_2/Al_2O_3 molar ratios (Table 1). The addition of a small amount of LiOH to the gel (sample G) produced single crystals. The possible roles for LiOH might include pH adjustment and mineralization. Although single crystals could also be obtained by increasing the ratio of GeO_2/Al_2O_3 in the presence of TMAOH, these were mostly twinned and highly aggregated. A Ge/Al = 1 has been observed for many of the aluminogermanate frameworks including the two GIS.[5] The highly basic solution (pH ⩾ 12) used in these syntheses to dissolve GeO_2 results in a tendency toward ordering as pointed out by Barrer and Zhdanov for low silica AlSi frameworks.[23,24]

Ion-Exchange Studies of K−AlGe-GIS. The crystal structure was determined only for an ca. 50% exchanged K form, (K, Na)−AlGe-GIS. Crystals of fully Na-exchanged and NH_4 forms were highly mosaic and unsuitable for diffraction studies. The XRD pattern of the fully Na-exchanged K−AlGe-GIS shows a phase similar to that of the as-synthesized form of Na−AlGe-GIS, indicating an order−disorder transformation at a level greater than 50% Na exchange. The powder X-ray pattern of the NH_4-exchanged form indicates another distorted form of GIS topology.

The overall structure of (K, Na)−AlGe-GIS is similar to the parent structure, K−AlGe-GIS. All of the extraframework sites Na1, K1, OW1, and OW2 are

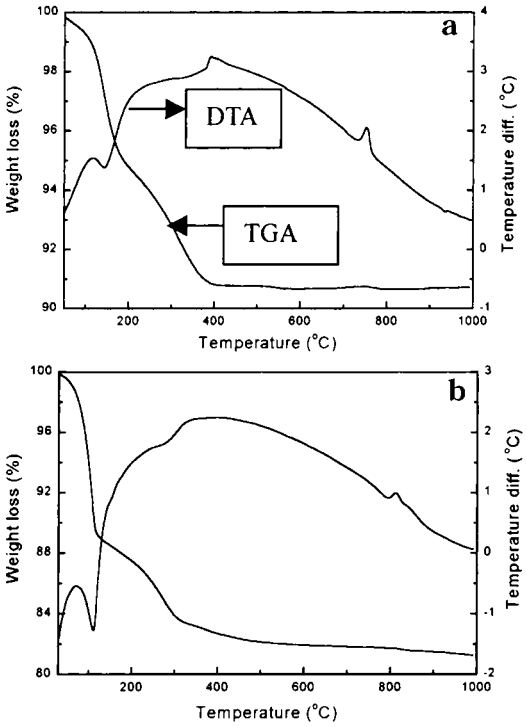

Figure 6. Thermogravimetry curves for (a) K−AlGe-GIS and (b) Na−AlGe-GIS. A heating rate of 10 °C/min in nitrogen flow was used for all of the measurements.

disordered with a statistical distribution. The sites K1 and OW2 are at the center of the eight-ring channels parallel to [100], whereas the sites Na1 and OW1 are nearly at the center of the eight-ring channels parallel to [001] (Figure V given as Supporting Information). The Na1 site is coordinated to four framework oxygen sites and to two water sites. The Na1−O distances range from 2.72(1) to 2.93(1) Å. Because the two disordered water sites are 5.134 Å apart, a coordination sphere of 6 can be assigned to Na1. The site K1 is coordinated to five framework oxygen sites and to two half-occupied water sites with bond distances ranging from 2.73(1) to 3.163(5) Å. Based on the arguments similar to those described for Na1, a coordination sphere of 7 can be assigned to K1. Crystallographic results for (K, Na)−AlGe-GIS are given in Table 2, while atomic coordinates and anisotropic displacement parameters are given in Table II (given as Supporting Information). A full list of bond lengths, bond angles, and observed and calculated structure factors can be obtained from authors.

Thermal Analysis. The TGA/DTA results for K−AlGe-GIS and Na−AlGe-GIS are plotted in Figure 6a,b. For K−AlGe-GIS, there are two dehydration steps, one between RT and 200 °C accounting for the 5% weight loss and the other between 200 and 400 °C accounting for the 4% weight loss. The total loss matches closely the amount of H_2O (8.2%) in the framework determined by single-crystal structure analysis (Table 2). The DTA curve shows peaks at 150 and 400 °C, corresponding to the dehydration steps in the TGA curve. The peak at 400 °C indicates complete dehydration of K−AlGe-GIS without collapse of the GIS framework. The exotherm peak at 750 °C indicates the collapse of the GIS framework into a dense $KAlGeO_4$ phase (JCPDS 19-928) as confirmed by an ex situ powder diffraction study. The TGA curve for Na−AlGe-GIS shows four dehydration

(23) Barrer, R. M.; Mainwaring, D. E. *J. Chem. Soc., Dalton Trans.* **1972**, 1254.
(24) Zhdanov, S. P. *Molecular Sieves*; Society of Chemical Industry: London, 1968; p 70.

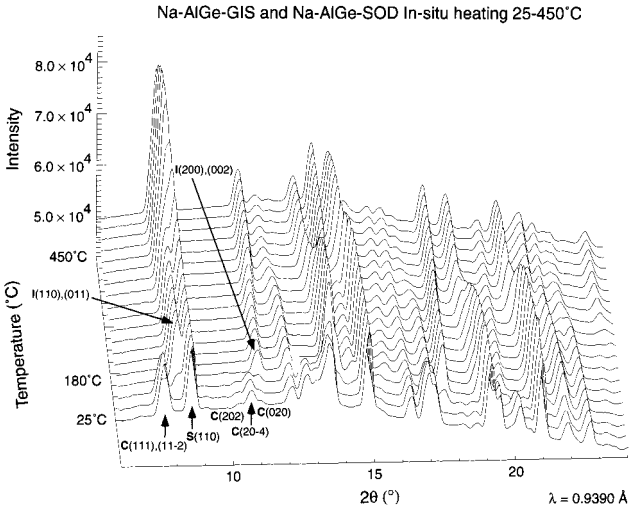

Figure 7. Plot of the synchrotron X-ray powder diffraction profiles as a function of temperature during the in situ heating of the sample J (Table 1). Letters C, I, and S represent *C*- and *I*-centered monoclinic cells from Na−AlGe-GIS and a primitive cubic cell from Na−AlGe-SOD, respectively.

steps, at RT to 120, 120−200, 200−380, and 380−520 °C, with 520 °C being the temperature of complete dehydration. The total weight loss is 18% and is 4.1% more than the amount of water (13.9%) calculated from the unit cell formula (Table 2). This extra loss can be assigned to water physically adsorbed on Na−AlGe-GIS. This is evident from comparison of the TG curves for the two AlGe frameworks. In the case of Na−AlGe-GIS, the weight loss of 3% up to 100 °C is higher than the 1% weight loss up to 100 °C in K−AlGe-GIS. The DTA curve shows a sharp endotherm at 110 °C and a broad endotherm between 260 and 340 °C corresponding to the dehydration steps in the TG curve. An exotherm at 800 °C corresponds to the collapse of Na−AlGe-GIS into a dense phase as confirmed by the ex situ powder diffraction pattern. This phase could not be identified with any of the existing $Na_{2z-3x-4y}Al_xGe_yO_z$ phases. The TGA/DTA curves for the completely Na-exchanged form of K−AlGe-GIS are similar to those for Na−AlGe-GIS as shown in Figure VI (given as Supporting Information).

The ex situ powder diffraction patterns confirm that both of the AlGe frameworks retain their structure up to ca. 750 °C. The overall dehydration behavior is similar to the dehydration process in (K, Na)−AlSi-GIS (amicite) and differs from that of other members of the GIS family, namely, gismondine and garronite.[6,22] The two AlGe frameworks do not collapse before complete dehydration, unlike gismondine and garronite. As pointed out by Vezzalini et al., this can be attributed to the presence of monovalent cations rather than the divalent Ca in gismondine and garronite, which have different coordination requirements.[22] Na−AlGe-GIS is thermally more stable than K−AlGe-GIS.

In Situ Synchrotron X-ray Powder Diffraction Studies. The difference between the structures of Na− and K−AlGe-GIS results from the ordering of cations in the eight-ring channel sites. We have noted site-specific ion-exchange mechanisms in zeolite X (LSX) with high ion-exchange capacity and the interrelationship between the extraframework site occupancy and

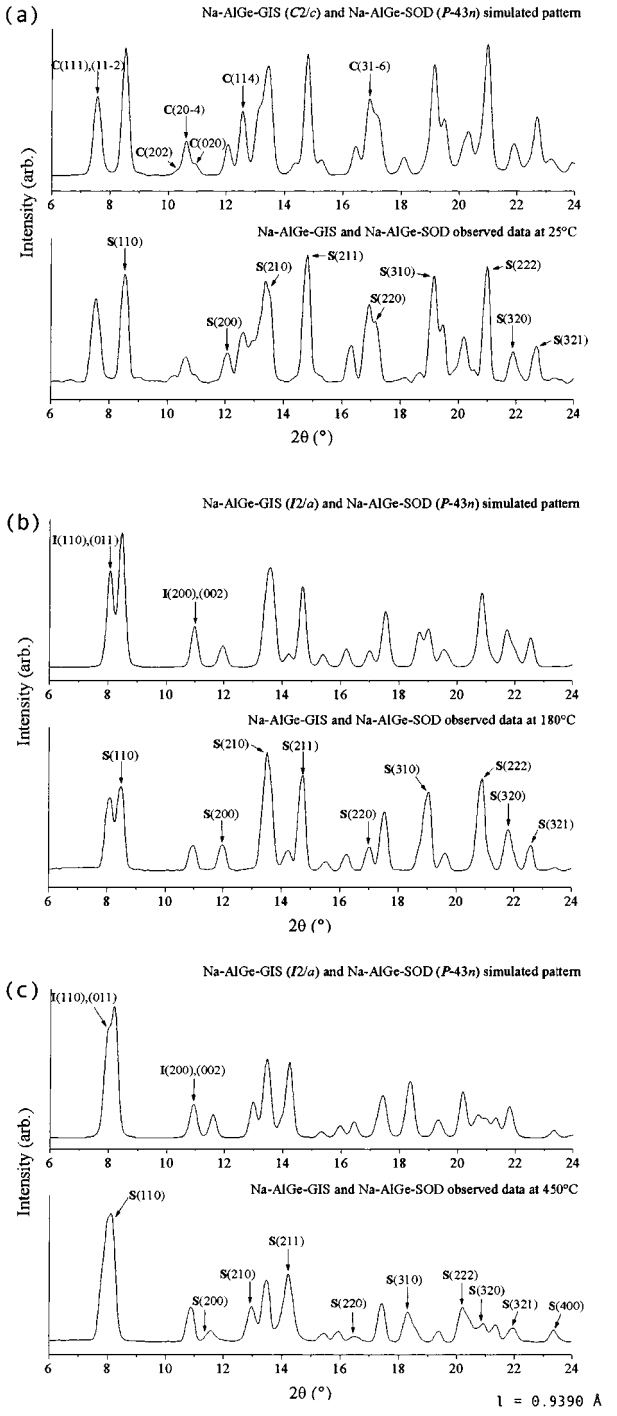

Figure 8. Observed and calculated powder diffraction patterns from the in situ data and DLS modeling (see text). All of the peaks from Na−AlGe-SOD are marked with their indices for comparison.

the structure.[25] In the case of AlGe-GIS, we suspect the change in structure from ordered (Na-*C*2/*c*) to disordered (K-*I*2/*a*) could be accompanied by ion exchange at some level more Na rich than $Na_{0.45}K_{0.55}$. Another strategy to observe this possible transition is through heating.

Time-resolved synchrotron X-ray powder diffraction patterns obtained during the in situ heating of Na−AlGe-GIS between 25 and 500 °C are shown in Figure 7. Two sets of peaks, which represent the *C*-centered

(25) Lee, Y.; Carr, S. W.; Parise, J. B. *Chem. Mater.* **1998**, *10*, 2561.

monoclinic cell from Na−AlGe-GIS and a primitive cubic cell from Na−AlGe−SOD, respectively, coexisted up to 150 °C. From this temperature to 180 °C, changes in the relative intensities and peak positions for the Na−AlGe-GIS phase were noticeable, as can be seen from the disappearance of the (111) and ($11\bar{2}$) doublet. The new sets of peaks are consistent with an *I*-centered cell. According to TGA, this period corresponds to the dehydration of Na−AlGe-GIS. The *I*-centered cell persisted up to the final temperature of 500 °C. The peaks from the Na−AlGe−SOD phase continued to shift to lower 2θ values throughout the in situ scan, indicating an increase in the cubic cell parameter as a function of temperature.

We suspected the observed transition from the *C*-centered to the *I*-centered cell for Na−AlGe-GIS was indicative of the disordering of Na cations upon heating. To confirm this speculation, powder diffraction patterns were generated for three selected models representing the phases at 25, 180, and 450 °C from the in situ data. DLS-optimized frameworks[26] were generated using the cell parameters determined from the in situ data. Prescribed T−O, O−O, and T−T distances were used assuming ideal AlO_4^{5-} and GeO_4^{4-} tetrahedra. A T−O−T angle of 135° was also used based upon the observations in AlGe analogues.[5a−h] For the simulation of the powder diffraction data, the results of the DLS-minimized framework were combined with the refined models for Na distribution: ordered Na sites from the Na−AlGe-GIS model and disordered Na sites from the K−AlGe-GIS model (Table 3). No H_2O groups were included in any of the simulations. The model for the Na−AlGe−SOD byproduct was also calculated in a similar fashion. Figure 8 shows the observed and calculated powder diffraction patterns at 25, 180, and 450 °C. The fits to the observed data are reasonable, despite the positions of the disordered Na sites not being adjusted from the values expected for K−AlGe-GIS. These results suggest that a gradual transition from the *C*-centered to the *I*-centered cell involving disordering of the Na cation occurs from 150 to 180 °C in Na−AlGe-GIS.

Conclusions

Single crystals of two aluminogermanate materials with the GIS topology have been grown for the first time and their structures determined. A unique ordered distribution of Na sites is observed for Na−AlGe-GIS. This gives rise to *C*2/*c* symmetry and to a unit cell that has not been previously observed for the GIS topology. In contrast, a completely disordered distribution of K and H_2O sites in the perpendicular eight-ring channels is observed for K−AlGe-GIS, giving rise to *I*2/*a* symmetry and to a unit cell, which is common in GIS-type materials. Analysis of time-resolved synchrotron X-ray powder diffraction patterns obtained during the in situ heating of Na−AlGe-GIS indicates disordering of Na cations during one of the steps in the dehydration process, resulting in an *I*-centered monoclinic cell similar to that for K−AlGe-GIS at RT. A 50% ion exchange of K with Na preserved the space group symmetry *I*2/*a* of the parent material with a minor increase in the unit cell volume. Both of the aluminogermanates show high thermal stability and retain the GIS topology up to ca. 750 °C. In line with other AlGe frameworks, the T−O−T angles in both Na and K forms are contracted compared to isotopic AlSi frameworks. A more buckled crankshaft chain and hence a more distorted framework structure is also observed for both of the aluminogermanates. This has been attributed to the observed unique, ordered Na arrangement near the walls of the eight-ring channels in Na−AlGe-GIS. Such an arrangement of K cations is ruled out in K−AlGe-GIS because they reside along the center of the eight-ring channels and an ordered arrangement would result in unacceptable bond distances among them.

Acknowledgment. This work was supported by the NSF through Grants DMR-9713375 and EAR-9724501, which funded the installation of the InXS facility at Stony Brook. Research carried out in part at the NSLS at BNL is supported by the U.S. Department of Energy, Division of Materials Sciences and Division of Chemical Sciences, Office of Basic Energy Sciences (Grant DE-AC02-98CH10886 for the X7B beamline). Special thanks to Jonathan C. Hanson of the X7B beamline of the NSLS for his help in data collection and useful discussions. S.J.K. is grateful for partial support from Korea Institute of Science and Technology (KIST) and Korea Science and Engineering Foundation (KOSEF).

Supporting Information Available: Tables of selected crystal data of various GIS-type topologies and atomic coordinates for (K, Na)−AlGe-GIS and figures of projections and polyhedral representations of K− and Na−AlGe-GIS and thermogravimetry curves for Na-exchanged K−AlGe-GIS. This material is available free of charge via the Internet at http://pubs.acs.org.

CM000459S

(26) McCusker, L. B.; Baerlocher, Ch.; Nawaz, R. *Z. Kristallogr.* **1985**, *171*, 281.